

Phosphorene, Antimonene, Silicene and Siloxene based Novel 2D Electrode Materials for Supercapacitors – A brief Review

*Sandhya Venkateshalu^a, Subashini G^a, Preetam Bhardwaj^a, George Jacob^a, Raja Sellappan^a,
Vimala Raghavan^a, Sagar Jain^{b,c}, Saravanan Pandiaraj^d, Varagunapandiyar Natarajan^e, Basem
Abdullah M Al Alwan^e, Mohammed Khaloofah Mola Al Mesfer^e, Abdullah Alodhayb^f, Mohamad
Khalid^g and Andrews Nirmala Grace^{a*}*

^aCentre for Nanotechnology Research, Vellore Institute of Technology (VIT), Vellore 632014 Tamil Nadu, India.

^bAdvanced Materials Centre, School of Engineering, London South Bank University, 103, Borough Road, London, SE10AA UK

^cConcentrated Solar Power Center for Renewable Energy Systems, School of Water Energy and Environment, Cranfield University, Cranfield MK43 0AL, UK.

^dDepartment of Self Development Skills, CFY Deanship, King Saud University, Riyadh, Saudi Arabia

^eChemical Engineering Department, King Khalid University, Abha, Saudi Arabia-61421

^fResearch Chair for Tribology, Surface, and Interface Sciences, Department of Physics and Astronomy, College of Science, King Saud University, Riyadh 11451, Saudi Arabia

^gGraphene and Advanced 2D Materials Research Group, School of Engineering and Technology, Sunway University, Malaysia.

*Corresponding author mail ID: anirmalagladys@gmail.com; anirmalagrace@vit.ac.in;

Abstract

In the past decade, 2D materials such as graphitic carbon nitride, transition metal dichalcogenides, layered metal oxides and hydroxides, hexagonal boron nitride and MXenes have garnered a great attention with the discovery of graphene. Very recently, novel 2D materials analogous to graphene such as phosphorene, antimonene, silicene, siloxene, germanene etc., were discovered and are emerging as strong competitors to the existing 2D materials. These materials pose explicit properties making them suitable for various applications. This article reviews the properties, synthesis techniques and the supercapacitive nature of phosphorene, antimonene, silicene and siloxene while briefing the properties of other 2D materials viz. germanene, stanene, arsenene and bismuthene. With the successful implementation of phosphorene as supercapacitor electrode, research is progressing in exploring the supercapacitive nature of other novel 2D materials. The investigations on these materials are still in its infancy and most of the properties lack experimental evidence. The current research trends on these novel materials are discussed in this review.

Keywords: 2D materials; graphene, phosphorene, antimonene, supercapacitors

1. Introduction

With the increase in the global energy crisis, there is an increased need to explore novel energy resources and efficient energy storage systems [1]. The charge storage mechanisms and the kinetics happening at the interface of the electrode and the electrolyte govern the energy and power density of storage systems. In this regard, batteries are the widely used storage systems working on the principle of reversible redox reactions which exhibit increased energy density with low power density. Other innovative storage systems are supercapacitors, which exhibit increased power density and cycle life. The selection of electrode material plays an important role in improving the performance of supercapacitors [2, 3]. Various materials such as activated carbon, graphene, carbon nanotubes, metal oxides, metal nitrides, transition metal chalcogenides, conducting polymers and their composites have been explored as supercapacitor electrodes, with each of them exhibiting specific disadvantages and advantages with respect to the other [4-9]. Carbonaceous electrodes usually exhibit higher electrical conductivity and electrochemical stability; however, they suffer from poor cycle life and specific capacitance as they lack redox reactions [10]. Conducting polymer electrodes possess enhanced capacitance compared to carbonaceous materials while suffering from mechanical stress leading to poor stability [11]. Similarly, various metal oxides and composites that have been explored so far exhibit improved capacitance but face the issue of poor electrical conductivity [1, 12]. Research started to focus on exploring novel materials as supercapacitor electrodes, as electrode materials play the most important part in evaluating the performance of supercapacitor. Recently, two dimensional (2D) materials with thickness of few atoms have been gaining importance as supercapacitor electrodes. 2D electrode materials exhibit advantages such as (i) larger surface area (ii) the weak van der Waals forces acting between the layers help in the intercalation of electrolyte ions, and (iii) high

flexibility and mechanical strength exhibited by the materials enable them to be used as flexible electrodes [13]. The excellent thermal, electronic, mechanical and optical properties exhibited by graphene, discovered through a ‘scotch tape’ method by Geim and Novoselov in 2004 led to the extensive use of graphene in various fields [14-16]. Thus, the outstanding properties of graphene directed the research to progress in discovering various other 2D materials. The properties such as strong quantum confinement, tunable thickness, electrical conductivity and large surface area observed in 2D materials make them unique compared to materials of other dimensions [17]. The schematic representation of the performance comparison of 2D electrodes with 0D, 1D or 3D electrodes in energy storage is shown in **Figure 1**. 2D materials such as transition metal dichalcogenides (MoS_2 , WS_2 , WSe_2 , MoSe_2 and MoTe_2)[18], hexagonal boron nitride [19], graphitic carbon nitride [20], metal oxides and hydroxides [21] and MXenes [22] gained importance after graphene.

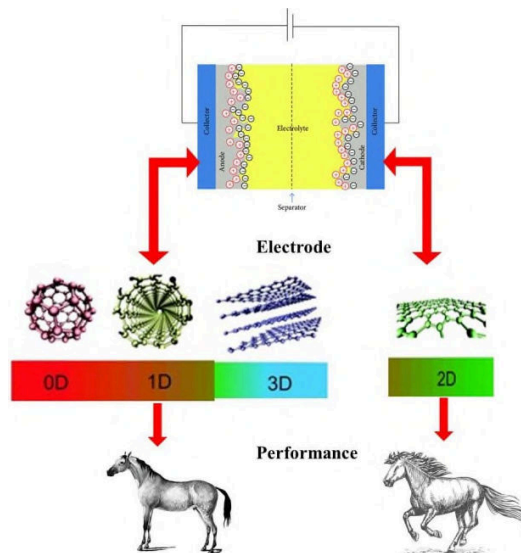


Figure 1. Graphical representation of the performance of 2D electrodes compared to other materials.

Very recently, novel 2D materials such as silicene, germanene, stanene, phosphorene, siloxene, arsenene, antimonene and bismuthene have attracted much attention due to their structures and properties analogous to graphene [23, 24]. The research trend in 2D materials since the discovery of graphene in 2004 is depicted in **Figure 2**. These novel 2D materials are usually synthesized through prominent techniques such as molecular beam epitaxy (MBE), mechanical and chemical exfoliations, chemical vapour deposition (CVD), ion intercalation and exfoliation techniques [24-26].

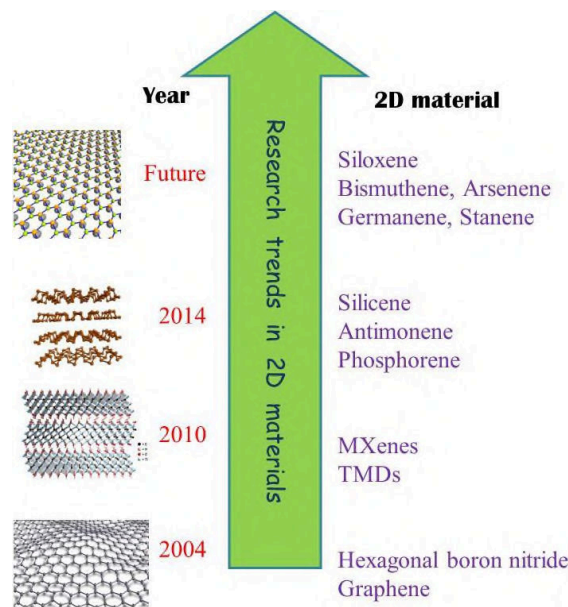


Figure 2. Research trends in 2D nanomaterials.

Though graphene is known to possess high electronic conductivity when compared to silicon; it is not a semiconductor which makes it difficult to be used in certain electronic applications. The novel 2D materials such as silicene, phosphorene and germanene have thus become strong competitors among 2D materials with their nature similar to graphene [23]. Though the experimental analysis on these materials are still in their infancy, we tried to summarize the current research trends on these materials as we hope that these are the future 2D materials. 2D materials are generally explored in energy storage applications due to their layered structures with well-

defined geometry, extreme hardness, capability to accommodate various intercalants, high mechanical strength, good chemical stability and large surface area. The high surface area of these novel 2D materials helps in improving the double-layer capacitance while the reactive basal planes and edges helps to improve the pseudocapacitance. Also the ion intercalation happening in the 2D materials makes them as promising electrode materials for supercapacitors [27]. With the success found in experimental evaluation of the supercapacitive nature of phosphorene, scientists gained interest in exploring the rest of Group VA elements such as arsenene, antimonene and bismuthene [28].

Though much report does not exist on the supercapacitive performance of these novel materials, a few available reports are summarized in this review.

2. Novel supercapacitor electrode materials

2.1 Phosphorene

Bridgman reported the synthesis of black phosphorous (BP) for the first time in 1914 from white phosphorous at high temperature and pressure [29]. Since then, not much interest was paid on black phosphorous until the discovery of 2D black phosphorous in 2014. In 2014, 2D black phosphorous named as phosphorene was proposed by mechanical exfoliation from its parent material using a blue tape method. This isolated single layer of black phosphorous was named as phosphorene as it is analogous to graphene [30]. The in-plane bonding in phosphorene is sp^3 hybridized due to which it exhibits a puckered structure unlike graphene [31]. The layers in phosphorene are held weakly through Van der Waals forces [32]. It possesses a band gap of 1.5 eV, which is greater than that of its bulk form (0.3 eV) [33]. Phosphorene is a semiconducting material with a hole mobility of $1000 \text{ cm}^2/\text{Vs}$ and is highly sensitive to an external electric field. The exciting fact about phosphorene is that its band gap decreases with an increase in 2D layer

spacing thus enabling them to have a tunable band gap [34, 35]. In the last five years, there are several evaluation works centered on the advancement concerning the useful functions of black phosphorus and phosphorene in different energy devices. **Figure 3** is a schematic illustration that represents the important role of phosphorene in electrochemical energy storage and imitates the growing research of phosphorene in energy storage applications. Recently, like a promising and potential 2D material, phosphorene has engrossed a lot of significance in the major fields and areas of materials science and electrochemistry [34, 35]. Due to the distinctive furrowed 2D configuration, phosphorene has a huge surface area, elevated carrier mobility and well-built mechanical strength (95 GPa) that are positive possessions in the field of energy harvesting and device renovation [35].

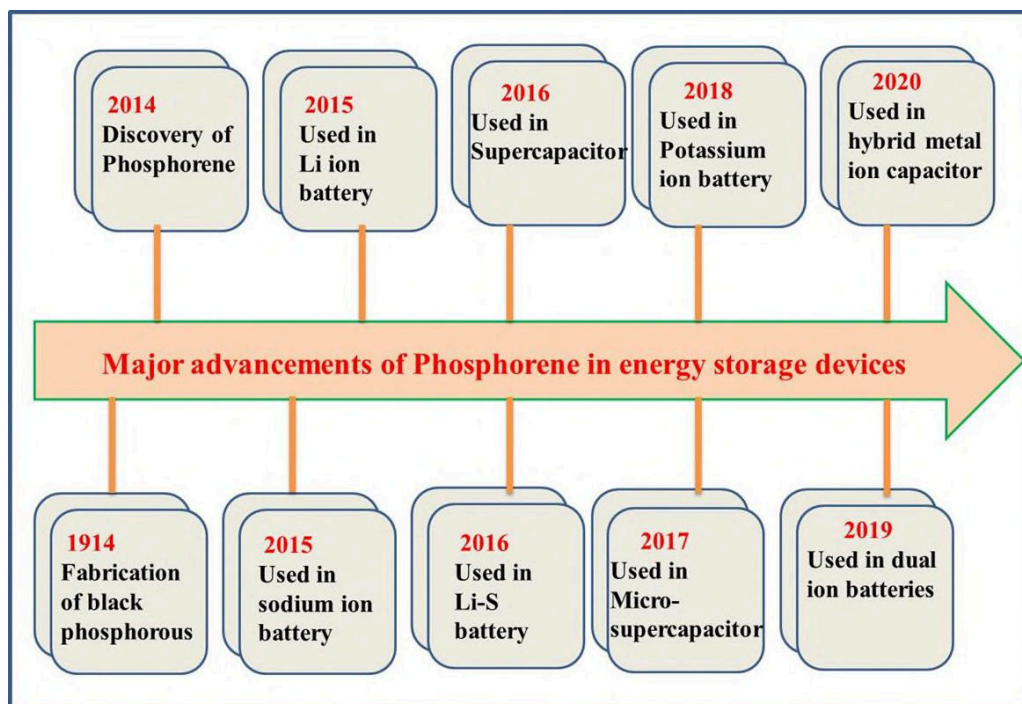


Figure 3. A schematic illustration of the major advancements of phosphorene in energy storage. Bulk black phosphorous is considered as a van der Waals material and thus the synthesis techniques employed in the production of graphene from graphite can also be applied to produce

phosphorene. Few layer thick phosphorene can be obtained by mechanical, liquid exfoliation, electrochemical exfoliation, pulsed laser deposition and plasma thinning techniques [36-41].

Table 1 summarizes the major methods used for the synthesis of phosphorene.

Table 1 Concise summary of methods employed in the synthesis of phosphorene.

Top Down Synthesis		Bottom up Synthesis	
Synthesis Process	Nature of product obtained	Synthesis Process	Nature of product obtained
Mechanical exfoliation (scotch Tape)	Few layers [37]	Pulsed Laser deposition (Growth on substrate, high cost, controllable preparation of material)	Amorphous and few layer thick material [39]
Liquid phase exfoliation (Ultra-sonication and rotating blade. Simple, cost effective process)	Prone to defects [38]		
Electrochemical exfoliation (High Voltage, scalable production, cost effective)	Thick material [41]		

The solution stripping method has found to be the best one for the large-scale production of phosphorene [42]. Kang et al., reported the synthesis of 2D phosphorene through the solvent stripping method by placing black phosphorus in an ultrasonicator with ice water, operated at a power of 30 W. The ultrasonication was carried out in a dark argon atmosphere glove box. A yield of about 1 mg/ml was obtained, which was further centrifuged to obtain phosphorene. **Figure 4** shows the microscopy analysis of the solvent-exfoliated BP [43].

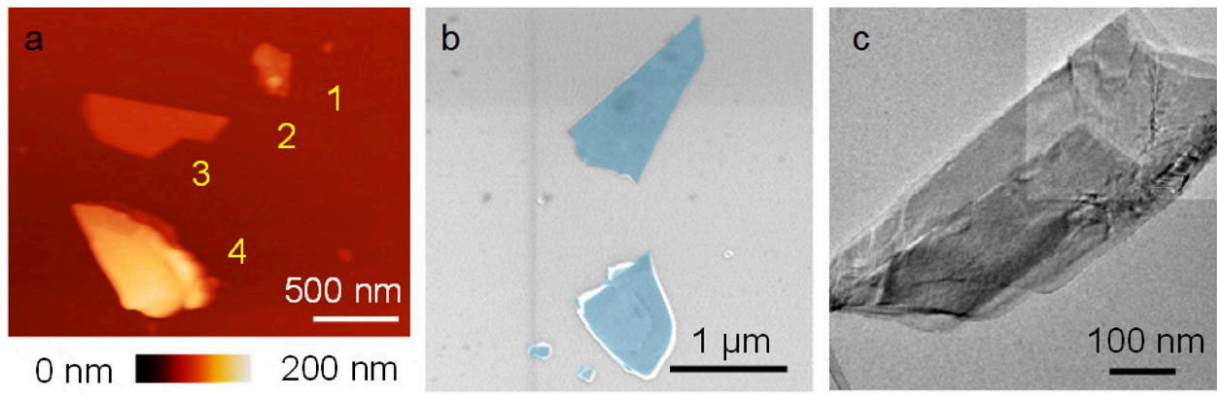


Figure 4. (a) AFM height image (b) false-colored SEM image (c) and low-resolution TEM image of solvent-exfoliated BP nanosheets. Adapted from Ref [43] copyright 2015 American Chemical Society.

The applications of phosphorene in various fields/devices are limited due to stability issues under ambient conditions. Phosphorene has two uncoupled pairs of electrons in each of its atoms, and it possesses a high surface to volume ratio, thereby making it highly reactive. Phosphorene easily reacts with oxygen, water and light and undergoes degradation to form oxidized phosphorous or phosphoric acid [44]. Phosphorous with a puckered structure exhibits good electrical conductivity and fast ion diffusivity making them suitable to be used as supercapacitor electrodes. Hao et al. reported the fabrication of a flexible supercapacitor using black phosphorous nanoflakes obtained through liquid phase exfoliation. Such a supercapacitor exhibited a specific capacitance of 59.3 F/g at 5 mV/s with capacitance retention of 71.8% after 30000 charge-discharge cycles [45].

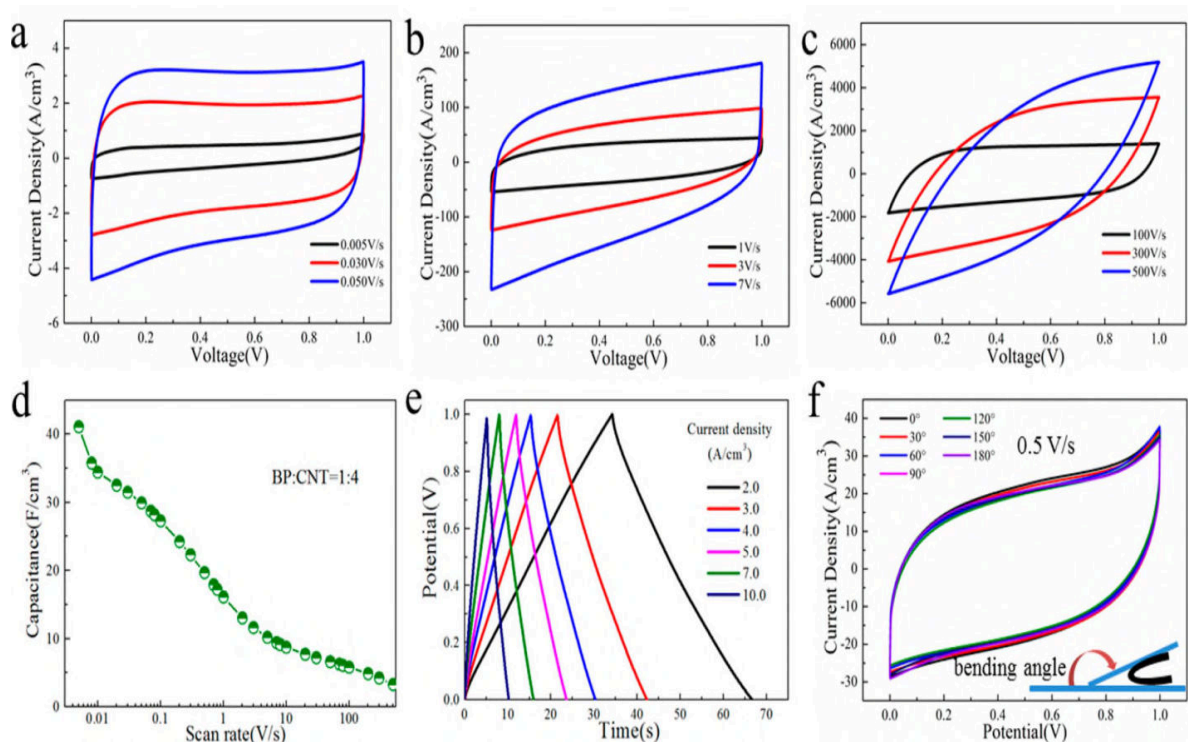


Figure 5. Electrochemical properties of BP/CNTs (1:4) ASSP device with $\sim 1.13 \mu\text{m}$ thick paper electrodes. (a-c) Cyclic voltammograms at various scan rates reach up to 500 V/s. (d) Stack capacitances calculated from the CV curves at different scan rates. (e) Galvanostatic charging/discharging curves at different current densities. (f) CV curves at a scan rate of 1 V/s with differently bent configurations. Adapted from Ref [46] copyright 2017 American Chemical Society.

Yang et al. reported the synthesis of BP/CNT nanocomposite and fabrication of a flexible supercapacitor. With BP/CNTs ratio of 1:4, the supercapacitor exhibited a capacitance of 41.1 F/cm^3 at 5 mV/s . The intercalation of CNTs into the BP layers helps in avoiding restacking of the BP layers. The electrochemical behavior of the flexible solid state device is shown in **Figure 5**. It has to be noted that the rectangular shape of the voltammogram slowly changes with the increase in the scan rate [46].

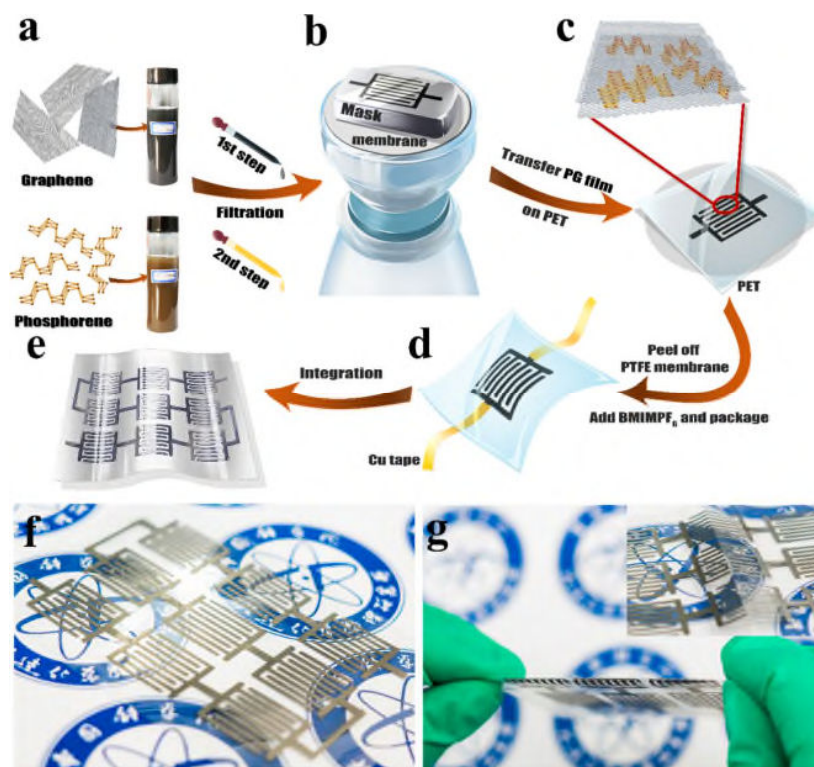


Figure 6. Mask-assisted simplified fabrication of PG-MSCs. (a-e) Illustration of the fabrication of PG-MSCs, which includes the following steps: (a) photograph of synthesized graphene and phosphorene inks; (b) step-by-step filtration of graphene and phosphorene in sequence with the assistance of an interdigital mask; (c) dry transfer of PG hybrid film onto PET substrate; (d) peeling off the PTFE membrane, drop-casting electrolyte, and device package; (e) integration of serially interconnected MSC devices. (f) Photograph of 9 serially interconnected PG-MSCs. (g) Flexibility and stability demonstration of PG interdigital electrodes at a highly folded state. Adapted from Ref [47] copyright 2017 American Chemical Society.

Xiao et al. demonstrated the fabrication of flexible micro supercapacitors through interdigital electrode patterning of phosphorene and graphene sheets layer on layer. The materials were transferred onto a polyethylene terephthalate (PET) substrate using a mask to produce a flexible electrode. When an ionic liquid such as 1-butyl methylimidazolium hexafluorophosphate

(BMIMPF₆) was used, the micro supercapacitor exhibited a specific capacitance of 9.8 mF/cm² with an energy density of 11.6 mWh/cm³. The schematic of the fabrication of phosphorene/graphene based micro supercapacitors is given in **Figure 6** [47]. Zu et al. reported the synthesis of phosphorene through an electrochemical cathodic exfoliation with a yield of ~93.1%. When used in an asymmetric hybrid system, the electrode exhibited an energy density of 203.7 W/kg [48]. Various reports on the application of black phosphorous and its composites as supercapacitor electrodes are available in literature [49-52].

Wen and his coworkers designed and fabricated black phosphorus sponge by employing electrochemical exfoliation technique for solid-state supercapacitor applications. The BP sponge was cut into small pieces and then spread over gold coated PET current collector after which, poly(vinylalcohol)/phosphoric acid (PVA/H₃PO₄) gel electrolyte was deposited over the BP sponge electrode and tested for its electrochemical activity. A schematic of the fabrication process and its electrochemical testing are illustrated in **Figure 7**. The pseudocapacitive nature was evaluated through cyclic voltammetry (CV) and galvanostatic charge/discharge (GCD) methods. From the CV curves, a specific capacitance of 80 F/g and 28 F/g was calculated at a scan rate of 10 mV/s and 100 mV/s, respectively. The GCD curves indicate the existence of double layer capacitance and the precise triangular shape indicates better charge transfer and diffusion between electrode/electrolyte interface. A 80% retention of capacitance even after 15,000 charge discharge cycles was observed which authenticates better reversibility response of the electrode material [53].

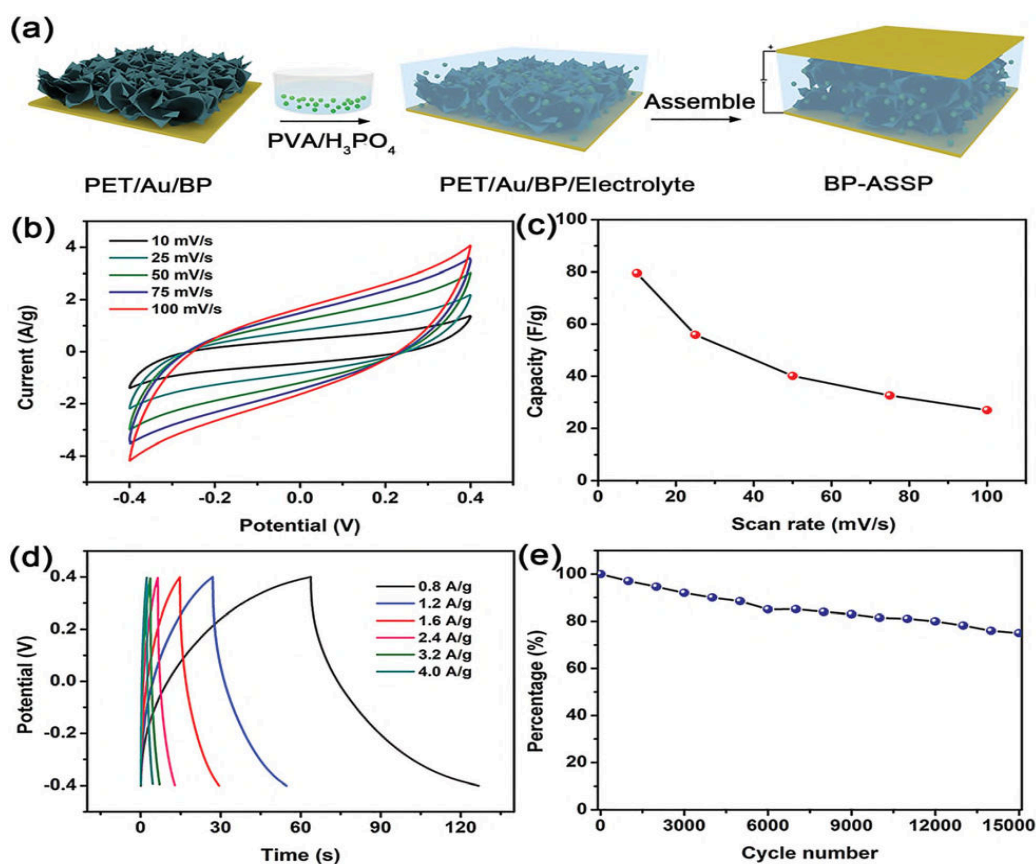


Figure 7. (a) Schematic illustration of the fabrication of BP sponge electrode (b) cyclic voltammograms obtained for various scan rates (c) mass capacitances calculated from the CV curves for various scan rates (d) galvanostatic charging/discharging curves obtained at different current densities and (e) cyclic stability test carried out for 15,000 cycles at a scanning rate of 100 mV/s . Adapted from Ref [53] copyright 2017 Royal Society of Chemistry.

Huang et al. reported the synthesis of anti self discharging phosphorene based zinc ion hybrid supercapacitor operating with a wide potential window. Two different electrolytes were used in evaluating the supercapacitive nature of the electrode. In “water in salt” electrolyte, the device exhibited a potential window of 2.2 V and a specific capacitance of 214 F/g, even after 5000 charge-discharge cycles. Authors found an extension in the operating potential window (2.5 V) of phosphorene based electrodes when an organic electrolyte (0.2 M Zinc chloride into the tetraethyl-

ammonium tetra-fluoro-borate in propylene carbonate ($\text{Et}_4\text{NBF}_4/\text{PC}$) is used. The device operating with this organic solvent exhibited a specific capacitance of 105 F/g even after 9500 charge discharge cycles. Additionally, this phosphorene based supercapacitor prominently acquire exceptional anti-self-discharge property. The phosphorene-Zinc ion based hybrid supercapacitor preserves 76% of capacitance even after 300 inactive hours. The authors established realistic function of the hybrid phosphorene metal ion based capacitor by utilizing a stretchy paper-based micro-capacitor. Authors claim that the phosphorene-zinc ion supercapacitor can efficiently solve the problem of the rigorous self-discharge difficulty found in ultracapacitors. Furthermore, metal ion phosphorene based capacitors operating at a high potential window are suitable for high power applications [54].

Zhao and his colleagues recently designed an innovative phosphorene embellished phase altered microcapsules that exhibit self-thermo regulatory property, which can be utilized as electrode material for ultracapacitors. The decline in electrochemical performance of ultracapacitors because of the high exothermic reaction during cycling process, lead to designing of self-thermo regulatory electrodes for future practical applications. Authors designed and developed these electrode materials for a wide temperature range. In this electrode material, the inner shell is comprised of n-docosane phase altered material embedded with silicon oxide, and the outer layer is coated with polyaniline/phosphorene hybrid structures that behave as a pseudocapacitive material. The electrode material reported in this work exhibits a distinctive blend of phosphorene and phase change material that demonstrates the prospective application of ultracapacitors at high temperatures [55].

Most recently, Kim et al. fabricated a hybrid nano-structured electrode material for supercapacitor that comprises of 2D functionalized phosphorene blended with conducting polymer, polypyrrole

(PPY). The hybrid electrode material was synthesized by a mechano-chemical method followed by an oxidative polymerization process, as illustrated in **Figure 8**. The authors investigated the polymerization process of pyrrole monomer on the surface of 2D phosphorene in detail. The obtained specific capacitance of hybrid electrode material was 411 F/g, which was four times higher when compared to pristine polypyrrole electrode material (106 F/g). Furthermore, the synthesized hybrid material enhanced the compositional durability of polypyrrole, comply the cyclic constancy of two times superior than that of immaculate polypyrrole. This is the first research publication on 2D phosphorene hybridized with conductive polymer for realistic use in energy-storage device [56].

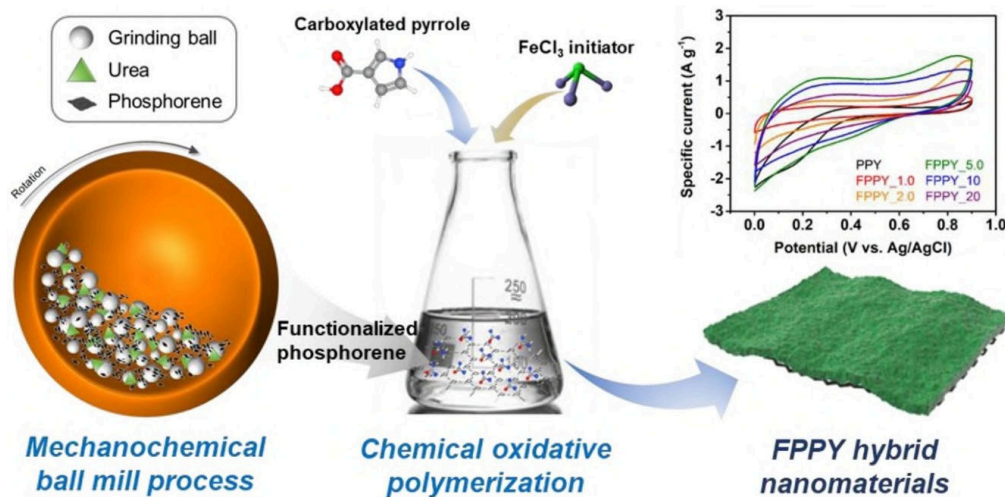


Figure 8. Schematic illustration depicting the formation of phosphorene-polypyrrole composite electrode material for supercapacitor application. Adapted from Ref [56] copyright 2020 Elsevier Ltd.

Hajibaba and Abdi evaluated the electrochemical properties of different phases of black, blue and green phosphorus by utilizing Joint Density Functional Theory (JDFT). Authors also investigated and calculated parameters such as charge density, energy density, band configuration and quantum capacitance for blue, black and green 2D phosphorus by employing JDFT. This work discussed

and observed the charge up intensity for different phases against different applied voltages. The obtained results were compared among all three phases blue, black and green 2D phosphorus. The outcome of the research investigation proposed that 2D phosphorous has superior areal capacitance compared with 2D graphene at elevated voltages [57].

2.2 Antimonene

The isolated few layers of black phosphorous had an appreciable band gap required for optoelectronic applications but were highly hygroscopic. They are highly sensitive to atmosphere and completely deteriorate upon exposure to air thereby limiting its practical applications [58]. This led to the search for new 2D materials with good stability and bandgap under atmospheric conditions. Antimony is a silvery lustrous, non-hygroscopic, layered material, which belongs to the same group as that of BP (group 15). It exhibits a band gap of 1.2 to 1.3 eV useful for optoelectronic applications [59]. Antimonene derived from crystals of antimony (Sb) can be obtained through techniques such as mechanical exfoliation, liquid phase exfoliation, and epitaxial growth and have found applications in various fields [60]. Ares et al. demonstrated the production of submillimeter flakes from a crystal of antimony by repeatedly peeling it using scotch tape and then pressing the tape against a Si (111) substrate. Thick flakes with many layers and low yield were obtained through this method. Thin flakes with large areas could be obtained by pressing the tape against a viscoelastic polymer coated glass slide and then pressing the slide against the substrate. Such flakes exhibited good stability for more than two months in atmospheric conditions [61]. Gusmao et al. reported the synthesis of antimonene through aqueous shear exfoliation using kitchen blades. A rotating blade was used to exfoliate the Sb crystals producing antimonene with sizes varying from 100 nm to 900 nm [62]. Gibaja et al. demonstrated the production of antimonene through liquid-phase exfoliation by sonicating antimony crystals in a mixture of 4:1 isopropanol

and water for 40 minutes. Non-exfoliated material was discarded through centrifugation, and the formation of layered antimonene was confirmed through AFM [63]. The electrochemical exfoliation of antimonene was reported by Lu et al., in which bulk antimony was used as cathode and Na_2SO_4 was used as the electrolyte. Upon application of a constant voltage of -6 V for 60 min, multilayered antimonene of 31.6 nm thickness was produced. Such an antimonene was stable upto 25 days in ambient conditions exhibiting higher stability to that of black phosphorous [64]. Molecular beam epitaxy (MBE) and van der Waals epitaxy (vdWE) are the widely used epitaxial growth techniques for producing high quality 2D layers. Ji et al. reported the use of vdWE for the synthesis of antimonene onto various substrates. A two zone (T1 and T2) furnace was used for this purpose in which antimony (Sb) powder was placed in T1 zone, which was subjected to heat to produce vapors of Sb. The vapors of Sb were passed to T2 zone, wherein the Sb atoms diffuse and crystallize onto the mica substrate. The schematic of setup, epitaxial growth process, optical and AFM images of the prepared samples are given in **Figure 9**. The antimonene formed exhibited a polygonal shape with a thickness of 4 nm (**Figure 9g**) [65].

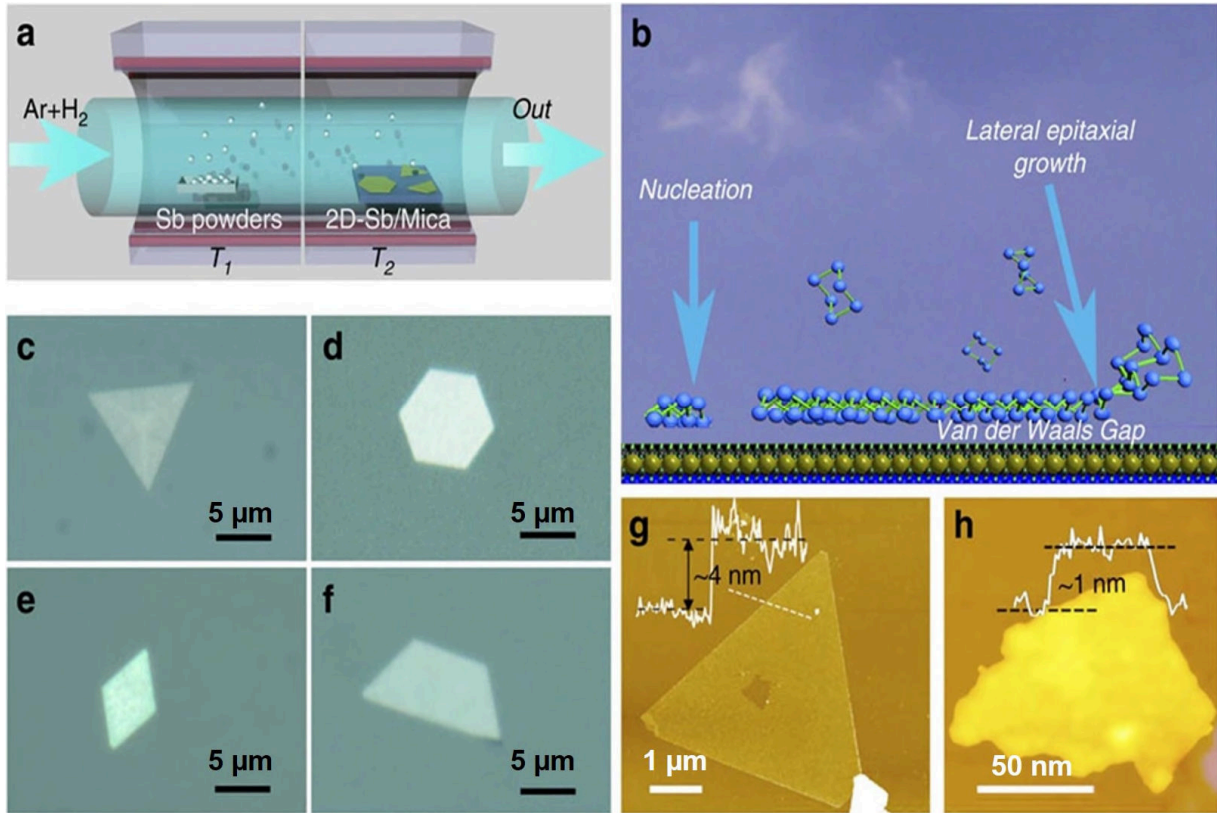


Figure 9. (a) A schematic illustration of the sample synthesis configurations (b) schematic of van der Waals epitaxy (c-f) Optical images of typical antimonene polygons with triangular, hexagonal, rhombic and trapezoidal shapes, respectively (g) AFM image of a typical triangular antimonene sheet (The thicknesses are 4 nm) (h) AFM image of a tiny antimonene sheet (The thickness is ca. 1 nm [65]).

Various reports exist on the demonstration of growth of antimonene onto different substrates such as PdTe₂, Ge (111), Bi₂Te₃ (111), Sb₂Te₃ (111) and Ag (111) using MBE techniques [66-68]. Experimental and theoretical studies have shown that the high surface area exhibited by antimonene (which is due to its puckered lamellar structure), large interlayer channel size (3.73 Å) and the good electrical conductivity (1.6×10^4 S/m) exhibited by them make them suitable candidates for energy storage applications [27]. Numerous reports exist on the use of antimonene electrodes in energy storage devices [69, 70]. Antimonene can be an excellent anode material in

Li and Na ion batteries as antimony exhibits a theoretical capacity of 660 mAh/g for storing both Li and Na ions [71]. Hou et al. reported the use of synthesized antimony/carbon fiber network as anode for sodium ion batteries. The electrode exhibited a capacity of 542 mAh/g at a high current density of 100 mA/g with a capacity retention of 96.7 % after 100 cycles [69]. Emiliano et al. reported the synthesis of antimonene by liquid phase exfoliation of antimony by sonicating it with isopropanol and tested for its supercapacitive nature. It exhibited a specific capacitance of 1578 F/g at a current density of 14 A/g. It was shown that with a slight increase in the content of antimonene onto the electrode by 1.8 to 36 ng, a significant increase in the capacitance could be obtained [27]. In the work reported by Mariappan et al., antimonene nanodendrites grown on Ni foam through electrochemical deposition process was used as a positive electrode in the construction of asymmetric supercapacitor (ASC) with graphene based negative electrode. The ASC exhibited energy and power density of 84.79 Wh/kg and 20625 W/kg respectively [28].

Ismail et al. reported that during the exfoliation of antimonene, the total surface area increases which lead to increase in the electrode active sites and electrolyte interactions thereby resulting in high specific capacitance of 597 F/g when compared to that of ball-milled antimony (101 F/g) at 10 mV/s. The impedance studies also showed low values of equivalence series resistance and charge transfer resistance compared to its bulk counterpart [72].

2.3 Silicene

Silicene synthesized by MBE methods on single crystals of Ag (111) at ultra-high vacuum has gained much attention with its graphene-like characteristics. This novel material was first reported in 2012 and has been a hot topic of research since then [73, 74]. These newly discovered 2D materials are similar to graphene only with respect to their 2D nature but vary invariably to graphene in different ways. Firstly, these materials do not have a 3D layered parent like graphene,

which can be exfoliated. They can only be synthesized chemically or through MBE techniques. The substrate on which it is grown greatly influences the structural and electronic properties of these 2D structures. The second difference is that, graphene is a fully flat material with sp^2 hybridization only, whereas group IV elements have a mixed sp^3 hybridization in their layers, which increases with an increase in its atomic size. This makes the bonds in the atoms to be buckled, resulting in non-flat layers. The buckling in the atoms of the newly discovered 2D elements is given in **Figure 10**. It can be seen that free-standing silicene has a buckling around 0.44 Å. The influence of the substrate and the buckling present in silicene greatly influences its properties enabling them to be used in electronic devices [75].

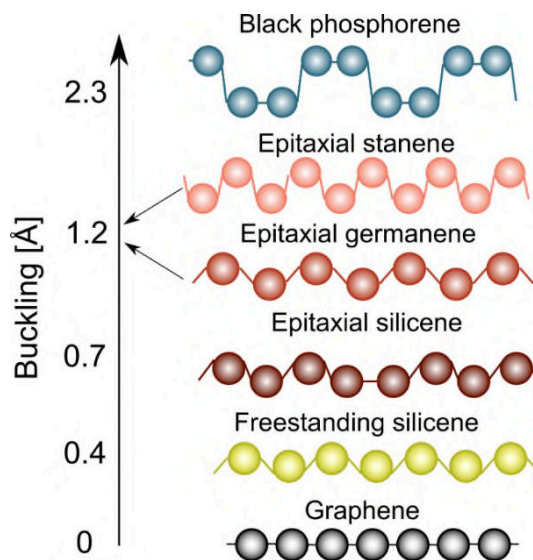


Figure 10. Illustration of the increasing buckling of different elemental 2D materials [76].

Mortazavi et al. reported the theoretical investigations of silicene on the storage capability of Na and Li ions. Based on their calculations, silicene could hold a capacitance of 954 mAh/g, which was much higher than that of germanene (369 mAh/g) and stanene (226 mAh/g) [77]. Zhang et al. reported the synthesis of silicene flowers through a simple chemical route, which was tested as anodes for Li-ion batteries. The silicene flowers consist of networks of silicene nanoplates with

different orientations forming a 3D flower-like structure. These electrodes exhibited a capacity of 2000 mAh/g at 800 mA/g with excellent rate capability [78]. The potential applications of silicene as supercapacitor electrodes were also explored by DFT computations [79-81]. It was shown that by introducing vacancy defects with doping (N, B, P and S) in silicene, the quantum capacitance of silicene electrodes could be enhanced. With an increase in the defect concentration, an increase in quantum capacitance was observed. With very low formation energies, S and B could bond strongly with Si atoms compared to P and N doped single vacancy silicene. These results show that silicene can be used as a supercapacitor electrode [80]. With the discovery of silicene, extensive research searched for new 2D materials synthesized through MBE under vacuum.

2.4 Siloxene

Most recently, two-dimensional silicon (Si) called siloxene has drawn more attention in energy storage devices such as lithium-ion batteries and supercapacitors. They are also used in biosensing applications such as dopamine sensors. Siloxene has been identified as a direct band gap material, discovered by German chemist Friedrich Wohler in 1863. Siloxene is synthesized through topotactic deintercalation of calcium and liquid exfoliation from Zintl phase of calcium silicide (CaSi_2). 2D siloxene acquire a squat buckled configuration owing to its dual band role position that is dissimilar from the graphene planar arrangement. The presence of surface terminating functional groups and mix up of sp^2 and sp^3 hybridization, enables siloxene to be used as electrode material in energy storage devices and in biomedical applications [82, 83]. Siloxene is produced by de-intercalation of Ca^{2+} from CaSi_2 using aqueous hydrochloric acid. In brief, specific amounts of CaSi_2 powder and HCl are stirred in ice bath under inert gas for 2-3 days as illustrated in **Figure 11**. During this reaction, the de-intercalation of Ca layers and functionalization of Si sheet would take place concurrently to produce siloxene [84, 85].

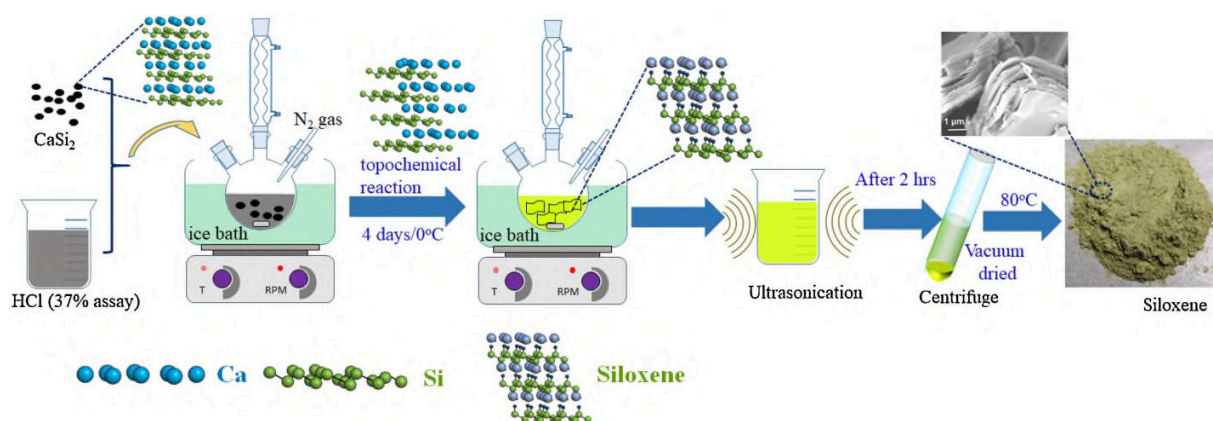


Figure 11. Synthesis process of 2D Siloxene novel material. Adapted from Ref [84] copyright 2020 Elsevier Ltd.

Based on parameters such as reaction period, acidic medium concentration and temperature used in the liquid exfoliation process, siloxene is identified as two types: Weiss and Kautsky siloxene configurations. Weiss type siloxene configuration written as $\text{Si}_6(\text{OH})_3\text{H}_3$ consist of six member rings that are Si_6 attached with substitute Si-OH and Si-H bonds while in Kautsky siloxene configuration written as $\text{Si}_6\text{O}_3\text{H}_6$ has Si_6 loop associated with Si-O-Si link.

The existence of bountiful functional groups on the surface of siloxene and its distinctive 2D configuration make siloxene useful in several applications especially as electrode materials for supercapacitors. Conversely, due to incomplete information of siloxene's electrochemistry, merely a small number of research efforts have been published and investigated on the electrochemical function of siloxene. The siloxene has been primarily engaged in supercapacitors and lithium-ion batteries as an electrode material and recognition of biomarkers in biomedical sensors technology [82, 83]. In 2018, Krishnamoorthy and his coworkers employed Siloxene as electrodes for symmetric supercapacitor abbreviated as SSC [82]. They reported the preparation of Kautsky siloxene configuration made by de-interspersion of calcium silicides through removal of calcium and define its Si-O-Si link with Si_6 rings and their inter-correlations by Fourier transform infrared

spectroscopy (FTIR). The pseudocapacitance behavior of 2D Siloxene has been evaluated in tetraethyl ammonium tetrafluoroborate (TEABF₄) organic electrolyte. The siloxene based symmetric supercapacitor exhibited interesting results with an operating potential window of 3 V. The constructed SSC device exhibit distinctive pseudocapacitive results with energy density and areal energy density of 5 Wh/Kg and 9.82 mJ/cm² respectively. The SSC device demonstrates nearly 98% retention of capacitance despite of 10000 charge-discharge cycles. The electron transport and dispersion rate of the electrolyte ions improved significantly due to the presence of conductive hexagonal silicon frameworks within 2D siloxene during the execution of electrochemical faradic reactions. The existence of large scale interlayer space between siloxene sheets and huge accessible surface area is responsible for quick ion transportation that leads to acquiring outstanding pseudocapacitance values of SSC device [82]. In 2019, Pazhamalai and coworkers studied and reported the effect of high-temperature on the properties of siloxene [86]. The presence of rich quantity of the oxygen functional groups on the edge, or basal surface leads to a decrease in conductivity of 2D siloxene sheets. Therefore, removal of O₂ groups causes an increase in conductivity as well as electrochemical active sites for redox reactions. In this regard, Pazhamalai et al. reported the elimination of O₂ groups from pristine siloxene designated as p-siloxene, through treating them at high temperature (900°C) and designated temperature treated siloxene as HT-Siloxene. The calcinations process at 900°C decayed O₂ groups from the edge or base planes of siloxene layers without disturbing its 2D structure. Higher conductivity was observed in HT-siloxene as compared to p-siloxene leading to better performance of HT siloxene. The obtained pseudocapacitance value of HT siloxene is 1.7 times more than p-siloxene. The HT-Siloxene based supercapacitor device exhibited a maximum energy density of 6.6 Wh/Kg, which is much higher than p-siloxene i.e. 3.8 Wh Kg⁻¹. The entire exclusion of O₂ groups from p-siloxene

improved the energy density of device. This also led to the increase in the cyclic stability of the device [86]. Kim and coworkers investigated another attractive approach by using siloxene coated nickel foam as a catalyst for dry restructuring methane (DRM). Carbon coated siloxene/Ni foam catalyst was then utilized as electrode material for supercapacitors. The schematic of this process is shown in **Figure 12** [87]. The carbon obtained through DRM reactions is deposited over siloxene coated nickel foam resulting in enhanced capacitance. In comparison with previously published works, carbon deposited siloxene/Ni foam composite reveals a much higher energy density of 30.8 WhKg^{-1} that shows an incredible improvement in pseudocapacitance values. This approach demonstrates the utilization of already used siloxene-based catalyst waste for energy storage and harvesting applications. More recently, Pazhamali and his co-workers analyzed and investigated the production of silicon-oxy-carbide (SiOC) by using the carbothermal decomposition process of siloxene sheets. This approach also authenticates the synthesis of a stretchy template from siloxene that can directly be utilized for supercapacitor application. Integration of siloxene with sodium alginate at 900°C led to the development of silicon-oxy-carbide (SiOC). Electrodes based on SiOC exhibited enhanced cyclic stability and specific capacitance compared to siloxene based electrodes. The SiOC based energy storage device exhibited an energy density of 21 Wh/kg , which is much superior than pristine-siloxene as per the earlier published reports. [88].

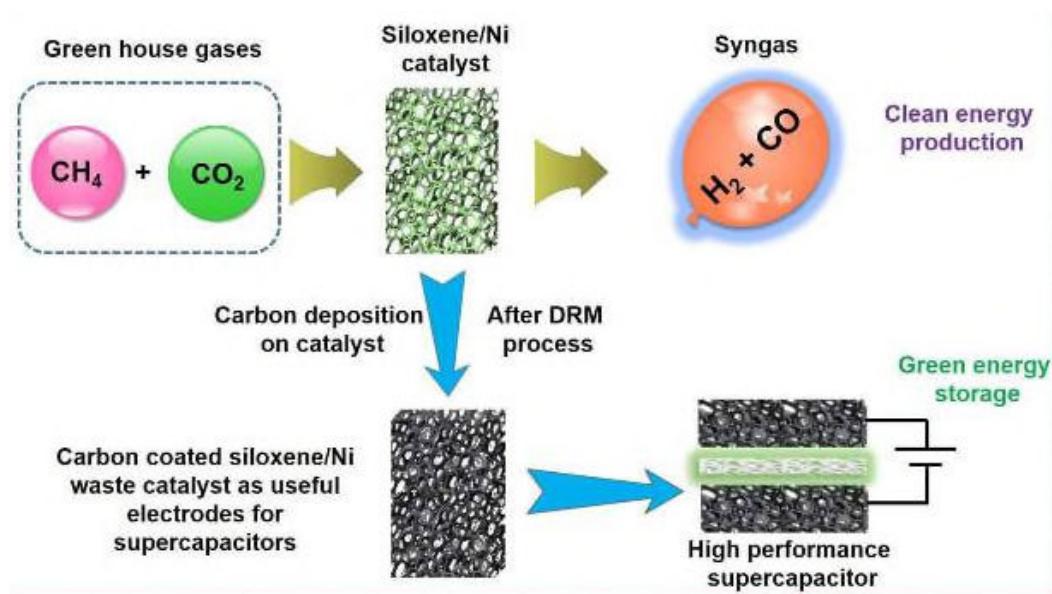


Figure 12. Graphic elucidation of the siloxene encrusted Ni foam was studied as a catalyst for the dry modification of methane (DRM) via the reaction between methane and carbon dioxide gases to generate syngas (H₂ + CO). The improved catalyst after DRM process shows the development or deposition of carbon on the surface due to methane disintegration and the recovered catalyst (carbon coated siloxene/Ni foam) is utilize as electrode for symmetric supercapacitor employing ionic liquid electrolyte. Adapted from Ref [87] copyright 2019 American Chemical Society.

Most recently, Krishnamoorthy et al. designed and developed a new hybrid electrode material, 2D/2D rGO-siloxene heterostructures for SCs device by de-intercalating calcium from CaSi₂ and partial reduction of graphene oxide via sonochemical reaction using hydrochloric acid as shown in **Figure 13** [89]. In this approach, an advanced electrode material is fabricated by hybridizing a 2D layer of rGO with a 2D layer of siloxene making a hetero-structure configuration. The double-layer capacitance from rGO integrates with the pseudocapacitance from siloxene resulting in the advanced performance of the device. An energy density of 56 Wh/Kg and power density of 15,000 WK/g was calculated from the device. The recently published research works centers on the synthesis of multi-component electrode materials for SCs devices [88, 89]. The synthesized rGO-

siloxene based supercapacitor can function over a broad temperature scale of -15 to 80 °C, making them appropriate for automobiles industry. These investigations demonstrate the real pertinence of siloxene-rGO electrode material to drive an electric car and capture the braking energy in regenerative brake-electric vehicle model. These efforts unlock innovative information for assessing the utilization of rGO-siloxene based SC as energy devices in electric automobiles.

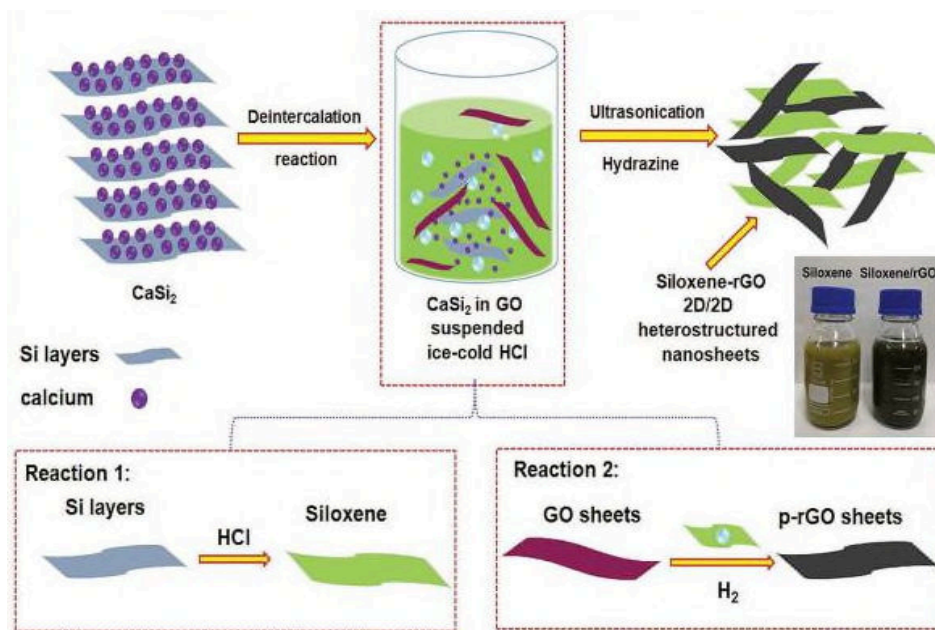


Figure 13. Graphical illustration of the synthesis of siloxene-rGO 2D/2D heterostructures.

Adopted from Ref [89] Copyright 2020 Wiley Publications

Composite electrode materials made with siloxene and rGO exhibit improved storage capability due to their synergistic effects. The specific capacitance of siloxene is limited due to its aggregation leading to an inferior precise surface area. Therefore, by establishing a spacer material such as transition metal oxides or carbon materials such as reduced graphene oxide (rGO) among the siloxene sheets, the admittance sites for the electrochemical reactions can be increased [90]. Meng and his colleagues have investigated supercapacitive performance by creating a three-dimensional

structural design of siloxene-reduced graphene oxide hydrogel (SGHG) by using an easy hydrothermal process as shown in **Figure 14** [90].

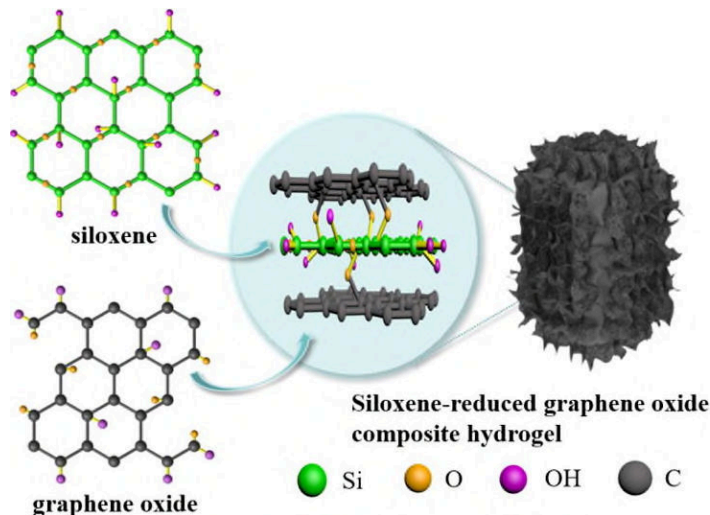


Figure 14. Schematic representing the fabrication of siloxene-reduced graphene oxide composite hydrogel (SGHG). Adapted from Ref [90] Copyright 2020 Elsevier Publications.

The fusion configuration of SGHG has improved the explicit surface area and better ion diffusion, resulting in enhanced capacitance. Pure siloxene electrode material exhibited a specific capacitance of 23 Fg^{-1} . With a current density of 1 Ag^{-1} , the composite SGHG with 1:3 ratio of the combined materials reveals a high specific capacitance of 520 Fg^{-1} via the synergistic effect of two components. The existence of oxygen functional groups on the surface of siloxene enhance the soaking ability of the electrode within electrolyte interface. They also offer pseudocapacitance resulting in an exceptional rate capability and capacitance retention [90].

2.5 Other novel 2D materials

Various other novel 2D materials such as germanene, stanene, bismuthene and arsenene have also started gaining attention with the success of phosphorene. However, the properties of these new novel materials are still not explored and sufficient details on them are still not reported in the literature [91-94]. In addition, these materials are yet to be explored as supercapacitor electrodes

while they are found to be useful in few other applications. With the discovery of silicene, germanene was synthesized by Bianco and his group [95]. Hydrogen terminated germanium sheets of millimeter-scale were synthesized from topochemical de-intercalation of CaGe_2 . The synthesized sheets were thermally stable and can be mechanically exfoliated as single or few-layered structures onto SiO_2/Si . It has a direct band gap of 1.53 eV, making them useful for optoelectronics and sensing applications. Wang et al., reported the use of Germanene nanoribbons in spin field effect transistor (FET) by first principle calculations, which proves that germanene will be the future hot material for spintronic [96]. Davila et al., reported the growth of one-atom thick germanene layers using MBE on Au (111) substrate, which was similar to the growth of silicene layers on Ag (111) substrates [97]. Zhu et al., demonstrated the use of silicene/germanene attached to MgX_2 ($X = \text{Cl}, \text{Br}$ and I) for Li ion storage applications through first-principle calculations [98]. However, the supercapacitive behavior of germanene is yet to be explored.

Stanene is the tin counterpart of graphene identified as a promising candidate in electronic device fabrication due to its tunable band gap and topological states [23]. Though there is a lack of knowledge on the basic properties of stanene, the similarities in their crystal and electronic structure to that of graphene has enabled them to be the hot topic of research. The successful synthesis of 2D stanene through MBE was reported by Zhu et al. for the first time and the formation was confirmed through STM [99]. Growth of stanene on Cu (111) at low-temperature was reported by Deng and his group. It was reported that stanene was ultra-flat that could be used for various electronic devices [93]. Bismuthene is the latest member of the 2D family with excellent optoelectronic and catalytic properties. Since bismuthene cannot be synthesized easily by mechanical exfoliation from bismuth, reports on bismuthene are rare. The acid-interaction and liquid phase exfoliation method was used by Yang et al., to synthesize 2D bismuthene successfully.

The synthesized material was used as an absorber to the mode-lock laser [94]. Bismuthene acts as a topological insulator at room temperature while other insulators usually work at very low temperatures [92]. Similarly, Arsenene is yet another very recent 2D material, which are the most stable allotropes of arsenic. They have an indirect band gap of 0.83 eV with a puckered layered structure like that of phosphorene [100]. Very recently Shah et al., reported the evidence for the existence of monolayer arsenene [101].

3. Summary and outlook

With the increase in demand for energy and the need to develop efficient storage devices, supercapacitors have been the interesting research topic. In the process of enhancing the energy density of supercapacitors, various electrode materials are being explored. After the discovery of the wonder material graphene, research went on in discovering various other 2D graphene-like materials. Very recently, novel materials analogous to graphene such as antimonene, phosphorene, silicene, siloxene, germanene, and so on came into limelight with their unique properties. These materials have a tunable band gap, which enables them to be used in various electronic devices. They are usually synthesized through MBE, mechanical and chemical exfoliations, CVD, ion intercalation and exfoliation techniques. Among all the latest 2D novel materials mentioned here, phosphorene have been gaining much research attention due to its well established synthesis techniques. The basic properties of these 2D novel materials have been assessed theoretically. However a few properties lack experimental evidence providing a greater scope for research in this field. Though these materials are semiconducting unlike graphene, they do not have van der Waals forces between the layers in their bulk form. This is a major drawback in synthesizing them as freestanding sheets. A few reports exist for the successful synthesis of freestanding sheets which are discussed in this review. The research carried out to explore the energy storage capability of

these novel 2D materials has been summarized in this review. The few available theoretical and experimental proofs for using these materials as supercapacitor electrodes are discussed here. Though major research is progressing on the improvement of supercapacitive nature of novel 2D materials theoretically, there is not much experimental proof. Practical evidence is yet to be reported in detail for most of the novel 2D materials to be used as supercapacitor electrodes. With advancements and optimizations in the synthesis techniques, the novel 2D materials discussed in this review are sure to be the next generation materials useful for a myriad of applications.

Acknowledgment

The authors from King Khalid University thankful to the Scientific Research Deanship at King Khalid University for supporting this research through grant number RPG. 1/160/42.

References

- [1] F. Shi, L. Li, X.-l. Wang, C.-d. Gu, J.-p. Tu, Metal oxide/hydroxide-based materials for supercapacitors, *RSC Adv.* 4 (2014) 41910-41921. <https://doi.org/10.1039/C4RA06136E>.
- [2] A. González, E. Goikolea, J.A. Barrena, R. Mysyk, Review on supercapacitors: Technologies and materials, *Renew. Sustain. Energy Rev.* 58 (2016) 1189-1206. <https://doi.org/10.1016/j.rser.2015.12.249>.
- [3] L. Qin, Q. Tao, L. Liu, J. Jiang, X. Liu, M. Fahlman, L. Hou, J. Rosen, F. Zhang, Flexible Solid-State Asymmetric Supercapacitors with Enhanced Performance Enabled by Free-Standing MXene–Biopolymer Nanocomposites and Hierarchical Graphene–RuO_x Paper Electrodes, *Batter. Supercaps.* 3 (2020) 604-610. <https://doi.org/10.1002/batt.202000044>.
- [4] D. Han, J. Zhang, Z. Weng, D. Kong, Y. Tao, F. Ding, D. Ruan, Q.-H. Yang, Two-dimensional materials for lithium/sodium-ion capacitors, *Mater. Today Energy.* 11 (2019) 30-45. <https://doi.org/10.1016/j.mtener.2018.10.013>.

- [5] V. Sharma, I. Singh, A. Chandra, Hollow nanostructures of metal oxides as next generation electrode materials for supercapacitors, *Sci. Reports* 8 (2018) 1307. <https://doi.org/10.1038/s41598-018-19815-y>.
- [6] Y. Tan, Y. Liu, Z. Tang, Z. Wang, L. Kong, L. Kang, Z. Liu, F. Ran, Concise N-doped Carbon Nanosheets/Vanadium Nitride Nanoparticles Materials via Intercalative Polymerization for Supercapacitors, *Sci. Reports* 8 (2018) 2915. <https://doi.org/10.1038/s41598-018-21082-w>.
- [7] Y.S. Lim, C.W. Lai, S.B. Abd Hamid, Porous 3D carbon decorated Fe₃O₄ nanocomposite electrode for highly symmetrical supercapacitor performance, *RSC Adv.* 7 (2017) 23030-23040. <https://doi.org/10.1039/C7RA00572E>.
- [8] K. Ghosh, C.Y. Yue, M.M. Sk, R.K. Jena, S. Bi, Development of a 3D graphene aerogel and 3D porous graphene/MnO₂@polyaniline hybrid film for all-solid-state flexible asymmetric supercapacitors, *Sustain. Energy Fuels.* 2 (2018) 280-293. <https://doi.org/10.1039/C7SE00433H>.
- [9] Q. Meng, K. Cai, Y. Chen, L. Chen, Research progress on conducting polymer based supercapacitor electrode materials, *Nano Energy* 36 (2017) 268-285. <https://doi.org/10.1016/j.nanoen.2017.04.040>.
- [10] L. Hao, X. Li, L. Zhi, Carbonaceous Electrode Materials for Supercapacitors, *Adv. Mater.* 25 (2013) 3899-3904. <https://doi.org/10.1002/adma.201301204>.
- [11] G.A. Snook, P. Kao, A.S. Best, Conducting-polymer-based supercapacitor devices and electrodes, *J. Power Sources* 196 (2011) 1-12. <https://doi.org/10.1016/j.jpowsour.2010.06.084>.

- [12] X. Yun, J. Li, X. Chen, H. Chen, L. Xiao, K. Xiang, W. Chen, H. Liao, Y. Zhu, Porous Fe₂O₃ Modified by Nitrogen-Doped Carbon Quantum Dots/Reduced Graphene Oxide Composite Aerogel as a High-Capacity and High-Rate Anode Material for Alkaline Aqueous Batteries, *ACS Appl. Mater. Interfaces*. 11 (2019) 36970-36984. <https://doi.org/10.1021/acsami.9b12827>.
- [13] J. Cherusseri, D. Pandey, J. Thomas, Symmetric, Asymmetric, and Battery-Type Supercapacitors Using Two-Dimensional Nanomaterials and Composites, *Batter. Supercaps*. 3 (2020) 860-875. <https://doi.org/https://doi.org/10.1002/batt.201900230>.
- [14] K.S. Novoselov, A.K. Geim, S.V. Morozov, D. Jiang, Y. Zhang, S.V. Dubonos, I.V. Grigorieva, A.A. Firsov, Electric Field Effect in Atomically Thin Carbon Films, *Science* 306 (2004) 666-669. <https://doi.org/10.1126/science.1102896>.
- [15] M.J. Allen, V.C. Tung, R.B. Kaner, Honeycomb Carbon: A Review of Graphene, *Chem. Rev.* 110 (2010) 132-145. <https://doi.org/10.1021/cr900070d>.
- [16] W. Choi, I. Lahiri, R. Seelaboyina, Y.S. Kang, Synthesis of Graphene and Its Applications: A Review, *Crit. Rev. Solid State Mater. Sci.* 35 (2010) 52-71. <https://doi.org/10.1080/10408430903505036>.
- [17] J. Li, X. Yun, Z. Hu, L. Xi, N. Li, H. Tang, P. Lu, Y. Zhu, Three-dimensional nitrogen and phosphorus co-doped carbon quantum dots/reduced graphene oxide composite aerogels with a hierarchical porous structure as superior electrode materials for supercapacitors, *J. Mater. Chem. A*. 7 (2019) 26311-26325. <https://doi.org/10.1039/C9TA08151H>.
- [18] R. Lv, J.A. Robinson, R.E. Schaak, D. Sun, Y. Sun, T.E. Mallouk, M. Terrones, Transition Metal Dichalcogenides and Beyond: Synthesis, Properties, and Applications of Single- and

- Few-Layer Nanosheets, *Acc. Chem. Res.* 48 (2015) 56-64.
<https://doi.org/10.1021/ar5002846>.
- [19] L. Liu, J. Park, D.A. Siegel, K.F. McCarty, K.W. Clark, W. Deng, L. Basile, J.C. Idrobo, A.-P. Li, G. Gu, Heteroepitaxial Growth of Two-Dimensional Hexagonal Boron Nitride Templated by Graphene Edges, *Science* 343 (2014) 163-167.
<https://doi.org/10.1126/science.1246137>.
- [20] L. Kong, P. Song, F. Ma, M. Sun, Graphitic carbon nitride-based 2D catalysts for green energy: Physical mechanism and applications, *Mater. Today Energy*. 17 (2020) 100488.
<https://doi.org/10.1016/j.mtener.2020.100488>.
- [21] Z. Sun, T. Liao, Y. Dou, S.M. Hwang, M.-S. Park, L. Jiang, J.H. Kim, S.X. Dou, Generalized self-assembly of scalable two-dimensional transition metal oxide nanosheets, *Nat. Commun.* 5 (2014) 3813. <https://doi.org/10.1038/ncomms4813>.
- [22] Y. Sun, D. Chen, Z. Liang, Two-dimensional MXenes for energy storage and conversion applications, *Mater. Today Energy*. 5 (2017) 22-36.
<https://doi.org/https://doi.org/10.1016/j.mtener.2017.04.008>.
- [23] S. Balendhran, S. Walia, H. Nili, S. Sriram, M. Bhaskaran, Elemental Analogues of Graphene: Silicene, Germanene, Stanene, and Phosphorene, *Small* 11 (2015) 640-652.
<https://doi.org/10.1002/sml.201402041>.
- [24] M. Pumera, Z. Sofer, 2D Monoelemental Arsenene, Antimonene, and Bismuthene: Beyond Black Phosphorus, *Adv. Mater.* 29 (2017) 1605299.
<https://doi.org/10.1002/adma.201605299>.

- [25] R. Sahoo, A. Pal, T. Pal, 2D materials for renewable energy storage devices: Outlook and challenges, *Chem. Commun.* 52 (2016) 13528-13542. <https://doi.org/10.1039/C6CC05357B>.
- [26] M. Akhtar, G. Anderson, R. Zhao, A. Alruqi, J.E. Mroczkowska, G. Sumanasekera, J.B. Jasinski, Recent advances in synthesis, properties, and applications of phosphorene, *Npj 2D Mater. Appl.* 1 (2017) 5. <https://doi.org/10.1038/s41699-017-0007-5>.
- [27] E. Martínez-Periñán, M.P. Down, C. Gibaja, E. Lorenzo, F. Zamora, C.E. Banks, Antimonene: A Novel 2D Nanomaterial for Supercapacitor Applications, *Adv. Energy Mater.* 8 (2018) 1702606. <https://doi.org/10.1002/aenm.201702606>.
- [28] V.K. Mariappan, K. Krishnamoorthy, P. Pazhamalai, S. Natarajan, S. Sahoo, S.S. Nardekar, S.-J. Kim, Antimonene dendritic nanostructures: Dual-functional material for high-performance energy storage and harvesting devices, *Nano Energy* 77 (2020) 105248. <https://doi.org/10.1016/j.nanoen.2020.105248>.
- [29] P.W. Bridgman, TWO NEW MODIFICATIONS OF PHOSPHORUS, *J. Am. Chem. Soc.* 36 (1914) 1344-1363. <https://doi.org/10.1021/ja02184a002>.
- [30] A. Castellanos-Gomez, Black Phosphorus: Narrow Gap, Wide Applications, *J. Phys. Chem. Lett.* 6 (2015) 4280-4291. <https://doi.org/10.1021/acs.jpcclett.5b01686>.
- [31] A. Castellanos-Gomez, L. Vicarelli, E. Prada, J.O. Island, K.L. Narasimha-Acharya, S.I. Blanter, D.J. Groenendijk, M. Buscema, G.A. Steele, J.V. Alvarez, H.W. Zandbergen, J.J. Palacios, H.S.J. van der Zant, Isolation and characterization of few-layer black phosphorus, *2D Mater.* 1 (2014) 025001. <https://doi.org/10.1088/2053-1583/1/2/025001>.

- [32] S. Appalakondaiah, G. Vaitheeswaran, S. Lebègue, N.E. Christensen, A. Svane, Effect of van der Waals interactions on the structural and elastic properties of black phosphorus, *Phys. Rev. B.* 86 (2012) 035105. <https://doi.org/10.1103/PhysRevB.86.035105>.
- [33] Y. Akahama, S. Endo, S.-i. Narita, Electrical Properties of Black Phosphorus Single Crystals, *J. Phys. Soc. Japan.* 52 (1983) 2148-2155. <https://doi.org/10.1143/JPSJ.52.2148>.
- [34] J.S. Shaikh, N.S. Shaikh, S.R. Sabale, N. Parveen, S.P. Patil, Y.K. Mishra, P. Kanjanaboos, S. Praserthdam, C.D. Lokhande, A phosphorus integrated strategy for supercapacitor: 2D black phosphorus doped and phosphorus-doped materials, *Mater. Today Chem.* 21 (2021) 100480. <https://doi.org/10.1016/j.mtchem.2021.100480>.
- [35] X.-Y. Han, H. Morgan Stewart, S. Shevlin, R. Catlow, Z.X. Guo, Strain and Orientation Modulated Bandgaps and Effective Masses of Phosphorene Nanoribbons, *Nano Lett.* 14 (2014). <https://doi.org/10.1021/nl501658d>.
- [36] L. Li, Y. Yu, G.J. Ye, Q. Ge, X. Ou, H. Wu, D. Feng, X.H. Chen, Y. Zhang, Black phosphorus field-effect transistors, *Nat. Nanotechnol.* 9 (2014) 372-377. <https://doi.org/10.1038/nnano.2014.35>.
- [37] H. Liu, A.T. Neal, Z. Zhu, Z. Luo, X. Xu, D. Tománek, P.D. Ye, Phosphorene: An Unexplored 2D Semiconductor with a High Hole Mobility, *ACS Nano* 8 (2014) 4033-4041. <https://doi.org/10.1021/nn501226z>.
- [38] P. Yasaei, B. Kumar, T. Foroozan, C. Wang, M. Asadi, D. Tuschel, J.E. Indacochea, R.F. Klie, A. Salehi-Khojin, High-Quality Black Phosphorus Atomic Layers by Liquid-Phase Exfoliation, *Adv. Mater.* 27 (2015) 1887-1892. <https://doi.org/10.1002/adma.201405150>.

- [39] Z. Yang, J. Hao, S. Yuan, S. Lin, H.M. Yau, J. Dai, S.P. Lau, Field-Effect Transistors Based on Amorphous Black Phosphorus Ultrathin Films by Pulsed Laser Deposition, *Adv. Mater.* 27 (2015) 3748-3754. <https://doi.org/10.1002/adma.201500990>.
- [40] W. Lu, H. Nan, J. Hong, Y. Chen, C. Zhu, Z. Liang, X. Ma, Z. Ni, C. Jin, Z. Zhang, Plasma-assisted fabrication of monolayer phosphorene and its Raman characterization, *Nano Res.* 7 (2014) 853-859. <https://doi.org/10.1007/s12274-014-0446-7>.
- [41] L. Li, D. Zhang, J. Deng, Y. Gou, J. Fang, Electrochemical exfoliation of two-dimensional layered black phosphorus and applications, *J. Energy Chem.* 49 (2020) 365-374. <https://doi.org/10.1016/j.jechem.2020.03.010>.
- [42] D. Hanlon, C. Backes, E. Doherty, C.S. Cucinotta, N.C. Berner, C. Boland, K. Lee, A. Harvey, P. Lynch, Z. Gholamvand, S. Zhang, K. Wang, G. Moynihan, A. Pokle, Q.M. Ramasse, N. McEvoy, W.J. Blau, J. Wang, G. Abellan, F. Hauke, A. Hirsch, S. Sanvito, D.D. O'Regan, G.S. Duesberg, V. Nicolosi, J.N. Coleman, Liquid exfoliation of solvent-stabilized few-layer black phosphorus for applications beyond electronics, *Nat. Commun.* 6 (2015) 8563. <https://doi.org/10.1038/ncomms9563>.
- [43] J. Kang, J.D. Wood, S.A. Wells, J.-H. Lee, X. Liu, K.-S. Chen, M.C. Hersam, Solvent Exfoliation of Electronic-Grade, Two-Dimensional Black Phosphorus, *ACS Nano* 9 (2015) 3596-3604. <https://doi.org/10.1021/acs.nano.5b01143>.
- [44] A. Favron, E. Gaufrès, F. Fossard, A.-L. Phaneuf-L'Heureux, N.Y.W. Tang, P.L. Lévesque, A. Loiseau, R. Leonelli, S. Francoeur, R. Martel, Photooxidation and quantum confinement effects in exfoliated black phosphorus, *Nat. Mater.* 14 (2015) 826. <https://doi.org/10.1038/nmat4299>

- [45] C. Hao, B. Yang, F. Wen, J. Xiang, L. Li, W. Wang, Z. Zeng, B. Xu, Z. Zhao, Z. Liu, Y. Tian, Flexible All-Solid-State Supercapacitors based on Liquid-Exfoliated Black-Phosphorus Nanoflakes, *Adv. Mater.* 28 (2016) 3194-3201. <https://doi.org/10.1002/adma.201505730>.
- [46] B. Yang, C. Hao, F. Wen, B. Wang, C. Mu, J. Xiang, L. Li, B. Xu, Z. Zhao, Z. Liu, Y. Tian, Flexible Black-Phosphorus Nanoflake/Carbon Nanotube Composite Paper for High-Performance All-Solid-State Supercapacitors, *ACS Appl. Mater. Interfaces.* 9 (2017) 44478-44484. <https://doi.org/10.1021/acsami.7b13572>.
- [47] H. Xiao, Z.-S. Wu, L. Chen, F. Zhou, S. Zheng, W. Ren, H.-M. Cheng, X. Bao, One-Step Device Fabrication of Phosphorene and Graphene Interdigital Micro-Supercapacitors with High Energy Density, *ACS Nano* 11 (2017) 7284-7292. <https://doi.org/10.1021/acsnano.7b03288>.
- [48] L. Zu, X. Gao, H. Lian, C. Li, Q. Liang, Y. Liang, X. Cui, Y. Liu, X. Wang, X. Cui, Electrochemical prepared phosphorene as a cathode for supercapacitors, *J. Alloys Compd.* 770 (2019) 26-34. <https://doi.org/10.1016/j.jallcom.2018.07.265>.
- [49] X. Chen, G. Xu, X. Ren, Z. Li, X. Qi, K. Huang, H. Zhang, Z. Huang, J. Zhong, A black/red phosphorus hybrid as an electrode material for high-performance Li-ion batteries and supercapacitors, *J. Mater. Chem. A.* 5 (2017) 6581-6588. <https://doi.org/10.1039/C7TA00455A>.
- [50] Q. Peng, K. Hu, B. Sa, J. Zhou, B. Wu, X. Hou, Z. Sun, Unexpected elastic isotropy in a black phosphorene/TiC₂ van der Waals heterostructure with flexible Li-ion battery anode applications, *Nano Res.* 10 (2017) 3136-3150. <https://doi.org/10.1007/s12274-017-1531-5>.

- [51] S. Luo, J. Zhao, J. Zou, Z. He, C. Xu, F. Liu, Y. Huang, L. Dong, L. Wang, H. Zhang, Self-Standing Polypyrrole/Black Phosphorus Laminated Film: Promising Electrode for Flexible Supercapacitor with Enhanced Capacitance and Cycling Stability, *ACS Appl. Mater. Interfaces*. 10 (2018) 3538-3548. <https://doi.org/10.1021/acsami.7b15458>.
- [52] J. Pang, A. Bachmatiuk, Y. Yin, B. Trzebicka, L. Zhao, L. Fu, R.G. Mendes, T. Gemming, Z. Liu, M.H. Rummeli, Applications of Phosphorene and Black Phosphorus in Energy Conversion and Storage Devices, *Adv. Energy Mater.* 8 (2018) 1702093. <https://doi.org/10.1002/aenm.201702093>.
- [53] M. Wen, D. Liu, Y. Kang, J. Wang, H. Huang, J. Li, P.K. Chu, X.-F. Yu, Synthesis of high-quality black phosphorus sponges for all-solid-state supercapacitors, *Mater. Horizons*. 6 (2019) 176-181. <https://doi.org/10.1039/C8MH00708J>.
- [54] Z. Huang, A. Chen, F. Mo, G. Liang, X. Li, Q. Yang, Y. Guo, Z. Chen, Q. Li, B. Dong, C. Zhi, Phosphorene as Cathode Material for High-Voltage, Anti-Self-Discharge Zinc Ion Hybrid Capacitors, *Adv. Energy Mater.* 10 (2020) 2001024. <https://doi.org/10.1002/aenm.202001024>.
- [55] L. Zhao, Z. Sun, H. Wan, H. Liu, D. Wu, X. Wang, X. Cui, A novel self-thermoregulatory electrode material based on phosphorene-decorated phase-change microcapsules for supercapacitors, *Electrochim. Acta*. 354 (2020) 136718. <https://doi.org/10.1016/j.electacta.2020.136718>.
- [56] Y.K. Kim, K.-Y. Shin, Functionalized phosphorene/polypyrrole hybrid nanomaterial by covalent bonding and its supercapacitor application, *J. Ind. Eng. Chem.* 94 (2021) 122-126. <https://doi.org/10.1016/j.jiec.2020.10.044>.

- [57] S. Hajibaba, Y. Abdi, Two-dimensional phosphorus supercapacitors, *J. Energy Storage*. 33 (2021) 102062. <https://doi.org/10.1016/j.est.2020.102062>.
- [58] X. Ling, H. Wang, S. Huang, F. Xia, M.S. Dresselhaus, The renaissance of black phosphorus, *Proceedings of the National Academy of Sciences* 112 (2015) 4523-4530. <https://doi.org/10.1073/pnas.1416581112>.
- [59] S. Zhang, Z. Yan, Y. Li, Z. Chen, H. Zeng, Atomically Thin Arsenene and Antimonene: Semimetal–Semiconductor and Indirect–Direct Band-Gap Transitions, *Angew. Chemie Int. Ed.* 54 (2015) 3112-3115. <https://doi.org/10.1002/anie.201411246>.
- [60] X. Wang, J. Song, J. Qu, Antimonene: From Experimental Preparation to Practical Application, *Angew. Chemie Int. Ed.* 58 (2019) 1574-1584. <https://doi.org/10.1002/anie.201808302>.
- [61] P. Ares, F. Aguilar-Galindo, D. Rodríguez-San-Miguel, D.A. Aldave, S. Díaz-Tendero, M. Alcamí, F. Martín, J. Gómez-Herrero, F. Zamora, Mechanical Isolation of Highly Stable Antimonene under Ambient Conditions, *Adv. Mater.* 28 (2016) 6332-6336. <https://doi.org/10.1002/adma.201602128>.
- [62] R. Gusmão, Z. Sofer, D. Bouša, M. Pumera, Pnictogen (As, Sb, Bi) Nanosheets for Electrochemical Applications Are Produced by Shear Exfoliation Using Kitchen Blenders, *Angew. Chemie Int. Ed.* 56 (2017) 14417-14422. <https://doi.org/10.1002/anie.201706389>.
- [63] C. Gibaja, D. Rodríguez-San-Miguel, P. Ares, J. Gómez-Herrero, M. Varela, R. Gillen, J. Maultzsch, F. Hauke, A. Hirsch, G. Abellán, F. Zamora, Few-Layer Antimonene by Liquid-Phase Exfoliation, *Angew. Chemie Int. Ed.* 55 (2016) 14345-14349. <https://doi.org/10.1002/anie.201605298>.

- [64] L. Lu, X. Tang, R. Cao, L. Wu, Z. Li, G. Jing, B. Dong, S. Lu, Y. Li, Y. Xiang, J. Li, D. Fan, H. Zhang, Broadband Nonlinear Optical Response in Few-Layer Antimonene and Antimonene Quantum Dots: A Promising Optical Kerr Media with Enhanced Stability, *Adv. Opt. Mater.* 5 (2017) 1700301. <https://doi.org/10.1002/adom.201700301>.
- [65] J. Ji, X. Song, J. Liu, Z. Yan, C. Huo, S. Zhang, M. Su, L. Liao, W. Wang, Z. Ni, Y. Hao, H. Zeng, Two-dimensional antimonene single crystals grown by van der Waals epitaxy, *Nat. Commun.* 7 (2016) 13352. <https://doi.org/10.1038/ncomms13352>
- [66] T. Lei, C. Liu, J.-L. Zhao, J.-M. Li, Y.-P. Li, J.-O. Wang, R. Wu, H.-J. Qian, H.-Q. Wang, K. Ibrahim, Electronic structure of antimonene grown on Sb₂Te₃ (111) and Bi₂Te₃ substrates, *J. Appl. Phys* 119 (2016) 015302. <https://doi.org/10.1063/1.4939281>.
- [67] X. Wu, Y. Shao, H. Liu, Z. Feng, Y.-L. Wang, J.-T. Sun, C. Liu, J.-O. Wang, Z.-L. Liu, S.-Y. Zhu, Y.-Q. Wang, S.-X. Du, Y.-G. Shi, K. Ibrahim, H.-J. Gao, Epitaxial Growth and Air-Stability of Monolayer Antimonene on PdTe₂, *Adv. Mater.* 29 (2017) 1605407. <https://doi.org/10.1002/adma.201605407>.
- [68] Y. Shao, Z.-L. Liu, C. Cheng, X. Wu, H. Liu, C. Liu, J.-O. Wang, S.-Y. Zhu, Y.-Q. Wang, D.-X. Shi, K. Ibrahim, J.-T. Sun, Y.-L. Wang, H.-J. Gao, Epitaxial Growth of Flat Antimonene Monolayer: A New Honeycomb Analogue of Graphene, *Nano Lett.* 18 (2018) 2133-2139. <https://doi.org/10.1021/acs.nanolett.8b00429>.
- [69] H. Hou, M. Jing, Y. Yang, Y. Zhang, W. Song, X. Yang, J. Chen, Q. Chen, X. Ji, Antimony nanoparticles anchored on interconnected carbon nanofibers networks as advanced anode material for sodium-ion batteries, *J. Power Sources* 284 (2015) 227-235. <https://doi.org/10.1016/j.jpowsour.2015.03.043>.

- [70] W. Tian, S. Zhang, C. Huo, D. Zhu, Q. Li, L. Wang, X. Ren, L. Xie, S. Guo, P.K. Chu, H. Zeng, K. Huo, Few-Layer Antimonene: Anisotropic Expansion and Reversible Crystalline-Phase Evolution Enable Large-Capacity and Long-Life Na-Ion Batteries, *ACS Nano* 12 (2018) 1887-1893. <https://doi.org/10.1021/acsnano.7b08714>.
- [71] Z. Li, X. Tan, P. Li, P. Kalisvaart, M.T. Janish, W.M. Mook, E.J. Lubber, K.L. Jungjohann, C.B. Carter, D. Mitlin, Coupling In Situ TEM and Ex Situ Analysis to Understand Heterogeneous Sodiation of Antimony, *Nano Lett.* 15 (2015) 6339-6348. <https://doi.org/10.1021/acs.nanolett.5b03373>.
- [72] M. Mohamed Ismail, J. Vigneshwaran, S. Arunbalaji, D. Mani, M. Arivanandhan, S.P. Jose, R. Jayavel, Antimonene nanosheets with enhanced electrochemical performance for energy storage applications, *Dalton Transactions* 49 (2020) 13717-13725. <https://doi.org/10.1039/D0DT01753A>.
- [73] P. Vogt, P. De Padova, C. Quaresima, J. Avila, E. Frantzeskakis, M.C. Asensio, A. Resta, B. Ealet, G. Le Lay, Silicene: Compelling Experimental Evidence for Graphenelike Two-Dimensional Silicon, *Phys. Rev. Lett.* 108 (2012) 155501. <https://doi.org/10.1103/PhysRevLett.108.155501>.
- [74] B. Feng, Z. Ding, S. Meng, Y. Yao, X. He, P. Cheng, L. Chen, K. Wu, Evidence of Silicene in Honeycomb Structures of Silicon on Ag(111), *Nano Lett.* 12 (2012) 3507-3511. <https://doi.org/10.1021/nl301047g>.
- [75] S. Cahangirov, M. Topsakal, E. Aktürk, H. Şahin, S. Ciraci, Two- and One-Dimensional Honeycomb Structures of Silicon and Germanium, *Phys. Rev. Lett.* 102 (2009) 236804. <https://doi.org/10.1103/PhysRevLett.102.236804>.

- [76] P. Vogt, Silicene, germanene and other group IV 2D materials, *Beilstein J. Nanotechnol.* 9 (2018) 2665-2667. <https://doi.org/10.3762/bjnano.9.248>.
- [77] B. Mortazavi, A. Dianat, G. Cuniberti, T. Rabczuk, Application of silicene, germanene and stanene for Na or Li ion storage: A theoretical investigation, *Electrochim. Acta.* 213 (2016) 865-870. <https://doi.org/10.1016/j.electacta.2016.08.027>.
- [78] X. Zhang, X. Qiu, D. Kong, L. Zhou, Z. Li, X. Li, L. Zhi, Silicene Flowers: A Dual Stabilized Silicon Building Block for High-Performance Lithium Battery Anodes, *ACS Nano* 11 (2017) 7476-7484. <https://doi.org/10.1021/acsnano.7b03942>.
- [79] Q. Xu, G.M. Yang, X. Fan, W.T. Zheng, Adsorption of metal atoms on silicene: stability and quantum capacitance of silicene-based electrode materials, *Phys. Chem. Chem. Phys.* 21 (2019) 4276-4285. <https://doi.org/10.1039/C8CP05982A>.
- [80] G.M. Yang, Q. Xu, X. Fan, W.T. Zheng, Quantum Capacitance of Silicene-Based Electrodes from First-Principles Calculations, *J. Phys. Chem. C.* 122 (2018) 1903-1912. <https://doi.org/10.1021/acs.jpcc.7b08955>.
- [81] M.J. Momeni, M. Mousavi-Khoshdel, T. Leisegang, Exploring the performance of pristine and defective silicene and silicene-like XSi_3 ($X = Al, B, C, N, P$) sheets as supercapacitor electrodes: A density functional theory calculation of quantum capacitance, *Physica E: Low-dimensional Systems and Nanostructures* 124 (2020) 114290. <https://doi.org/10.1016/j.physe.2020.114290>.
- [82] K. Krishnamoorthy, P. Pazhamalai, S.-J. Kim, Two-dimensional siloxene nanosheets: novel high-performance supercapacitor electrode materials, *Energy Environ. Sci.* 11 (2018) 1595-1602. <https://doi.org/10.1039/C8EE00160J>.

- [83] R. Rajendran, Z.-x. Xu, F. Wang, Novel Two-Dimensional Siloxene Material for Electrochemical Energy Storage and Sensor Applications, in: K. Krishnamoorthy (Editor), Novel Nanomaterials, IntechOpen, 2020. <https://doi.org/10.5772/intechopen.93958>.
- [84] R. Ramachandran, X. Leng, C. Zhao, Z.-X. Xu, F. Wang, 2D siloxene sheets: A novel electrochemical sensor for selective dopamine detection, *Appl. Mater. Today*. 18 (2020) 100477. <https://doi.org/10.1016/j.apmt.2019.100477>.
- [85] H. Nakano, M. Ishii, H. Nakamura, Preparation and structure of novel siloxene nanosheets, *Chem. Commun.* (2005) 2945-2947. <https://doi.org/10.1039/B500758E>.
- [86] P. Pazhamalai, K. Krishnamoorthy, S. Sahoo, V.K. Mariappan, S.-J. Kim, Understanding the Thermal Treatment Effect of Two-Dimensional Siloxene Sheets and the Origin of Superior Electrochemical Energy Storage Performances, *ACS Appl. Mater. Interfaces*. 11 (2019) 624-633. <https://doi.org/10.1021/acsami.8b15323>.
- [87] K. Krishnamoorthy, S. M. S. P, P. Pazhamalai, V.K. Mariappan, Y.S. Mok, S.-J. Kim, A highly efficient 2D siloxene coated Ni foam catalyst for methane dry reforming and an effective approach to recycle the spent catalyst for energy storage applications, *J. Mater. Chem. A*. 7 (2019) 18950-18958. <https://doi.org/10.1039/C9TA03584B>.
- [88] P. Pazhamalai, K. Krishnamoorthy, S. Sahoo, V.K. Mariappan, S.-J. Kim, Carbothermal conversion of siloxene sheets into silicon-oxy-carbide lamellae for high-performance supercapacitors, *Chem. Eng. J.* 387 (2020) 123886. <https://doi.org/10.1016/j.cej.2019.123886>.
- [89] K. Krishnamoorthy, P. Pazhamalai, V.K. Mariappan, S. Manoharan, D. Kesavan, S.-J. Kim, Two-Dimensional Siloxene-Graphene Heterostructure-Based High-Performance

- Supercapacitor for Capturing Regenerative Braking Energy in Electric Vehicles, *Adv. Funct. Mater.* 31 (2021) 2008422. <https://doi.org/10.1002/adfm.202008422>.
- [90] Q. Meng, C. Du, Z. Xu, J. Nie, M. Hong, X. Zhang, J. Chen, Siloxene-reduced graphene oxide composite hydrogel for supercapacitors, *Chem. Eng. J.* 393 (2020) 124684. <https://doi.org/10.1016/j.cej.2020.124684>.
- [91] P. Vishnoi, M. Mazumder, S.K. Pati, C.N. R. Rao, Arsenene nanosheets and nanodots, *New J. Chem.* 42 (2018) 14091-14095. <https://doi.org/10.1039/C8NJ03186J>.
- [92] F. Reis, G. Li, L. Dudy, M. Bauernfeind, S. Glass, W. Hanke, R. Thomale, J. Schäfer, R. Claessen, Bismuthene on a SiC substrate: A candidate for a high-temperature quantum spin Hall material, *Science* 357 (2017) 287-290. <https://doi.org/10.1126/science.aai8142>.
- [93] J. Deng, B. Xia, X. Ma, H. Chen, H. Shan, X. Zhai, B. Li, A. Zhao, Y. Xu, W. Duan, S.-C. Zhang, B. Wang, J.G. Hou, Epitaxial growth of ultraflat stanene with topological band inversion, *Nat. Mater.* 17 (2018) 1081-1086. <https://doi.org/10.1038/s41563-018-0203-5>.
- [94] M.I. Khan, G. Nadeem, A. Majid, M. Shakil, A DFT study of bismuthene as anode material for alkali-metal (Li/Na/K)-ion batteries, *Mater. Sci. Eng. B.* 266 (2021) 115061. <https://doi.org/10.1016/j.mseb.2021.115061>.
- [95] E. Bianco, S. Butler, S. Jiang, O.D. Restrepo, W. Windl, J.E. Goldberger, Stability and Exfoliation of Germanane: A Germanium Graphane Analogue, *ACS Nano* 7 (2013) 4414-4421. <https://doi.org/10.1021/nn4009406>.
- [96] Y. Wang, J. Zheng, Z. Ni, R. Fei, Q. Liu, R. Quhe, C. Xu, J. Zhou, Z. Gao, J. Lu, Half-metallic silicene and germanene nanoribbons: towards high-performance spintronics device, *Nano* 07 (2012) 1250037. <https://doi.org/10.1142/S1793292012500373>.

- [97] M.E. Dávila, L. Xian, S. Cahangirov, A. Rubio, G. Le Lay, Germanene: a novel two-dimensional germanium allotrope akin to graphene and silicene, *New J. Phys.* 16 (2014) 095002. <https://doi.org/10.1088/1367-2630/16/9/095002>.
- [98] J. Zhu, A. Choneos, U. Schwingenschlögl, Silicene/germanene on MgX₂ (X = Cl, Br, and I) for Li-ion battery applications, *Nanoscale* 8 (2016) 7272-7277. <https://doi.org/10.1039/C6NR00913A>.
- [99] F.-f. Zhu, W.-j. Chen, Y. Xu, C.-l. Gao, D.-d. Guan, C.-h. Liu, D. Qian, S.-C. Zhang, J.-f. Jia, Epitaxial growth of two-dimensional stanene, *Nat. Mater.* 14 (2015) 1020-1025. <https://doi.org/10.1038/nmat4384>.
- [100] L. Ao, A. Pham, X. Xiang, F. Klose, S. Li, X. Zu, Tunable electronic and magnetic properties of arsenene nanoribbons, *RSC Adv.* 7 (2017) 51935-51943. <https://doi.org/10.1039/C7RA05137A>.
- [101] J. Shah, W. Wang, H.M. Sohail, R.I.G. Uhrberg, Experimental evidence of monolayer arsenene: an exotic 2D semiconducting material, *2D Mater.* 7 (2020) 025013. <https://doi.org/10.1088/2053-1583/ab64fb>.